CrossMark
click for updates

Electric field induced monoclinic phase in $(Na_{0.52}K_{0.48})(Nb_{1-y}Sb_y)O_3$ ceramics close to the rhombohedral-orthorhombic polymorphic phase boundary

Jian Fu,[1] Ruzhong Zuo,[1,a)] and Xingyu Gao[2]

[1]Institute of Electro Ceramics & Devices, School of Materials Science and Engineering, Hefei University of Technology, Hefei 230009, People's Republic of China
[2]Shanghai Synchrotron Radiation Facility, Shanghai Institute of Applied Physics, Chinese Academy of Sciences, Pudong New Area, Shanghai 201204, People's Republic of China

The electric field induced structural transformation in $(Na_{0.52}K_{0.48})(Nb_{1-y}Sb_y)O_3$ ceramics near the rhombohedral (R)-orthorhombic (O) phase boundary was investigated by means of ex-situ and in-situ synchrotron x-ray diffraction and dielectric measurements. An intermediate monoclinic (M) phase was irreversibly induced from the O phase by poling, leading to a modified polarization rotation path along R-M-O. By comparison, the reversibility of R-M phase transition would cause the phase instability. Both aspects were believed to be responsible for the high piezoelectric activity near the R-O phase boundary. Moreover, enhanced piezoelectric properties were also found to correlate with the thermal stability of the induced M phase. © 2013 AIP Publishing LLC.
[http://dx.doi.org/10.1063/1.4828713]

It is generally recognized that the phase coexistence (phase boundary) in ferroelectric materials should play a significant role in enhancing piezoelectric and electromechanical properties.[1,2] The relevant studies have been reported in conventional Pb-based piezoelectric materials such as $Pb(Zr,Ti)O_3$ (PZT) and $Pb(Mg_{1/3}Nb_{2/3})O_3$-$PbTiO_3$.[2–4] Some intermediate phases (IPs) were observed by means of high-resolution x-ray diffraction,[5–9] for example, the monoclinic (M) phase in PZT suggested by Noheda et al.[10] The finding of these intermediate phases provided a new method of viewing the rhombohedral (R)-tetragonal (T) (or T-R) phase transition.

$(Na,K)NbO_3$ (NKN) based lead-free materials have attracted much attention in the last ten years. Their excellent properties were believed to originate from the complex and tunable phase boundaries such as the classical morphotropic phase boundary (MPB) in NKN binary system[11,12] and the polymorphic phase boundary (PPB) in modified NKN systems.[13–15] The NKN ceramics were reported to own a successive polymorphic phase transition, which can be appropriately tuned,[13–19] such that the phase coexistence zone can be formed near room temperature. It is indicated that the addition of a small amount of Sb could help generate R-orthorhombic (O) phase coexisted NKN based lead-free ceramics, in which the piezoelectric constant d_{33} and mechanical coupling factor k_p reached their maxima.[18] It would be of much interest to know what is the mechanism of achieving significantly enhanced piezoelectric properties for Sb-doped NKN ceramics, although a few works have been initiated on other NKN-based compositions with initial O-T or R-T phase coexistence.[20–22]

In the present work, ex-situ and in-situ synchrotron x-ray diffraction measurements were carried out on unpoled and poled $(Na_{0.52}K_{0.48})(Nb_{1-y}Sb_y)O_3$ ($NKNS_y$) ceramics. Experimental evidences of the electric field induced irreversible O-M phase transition and reversible R-M phase transition (phase instability) were provided in combination with the dielectric measurements on unpoled and poled samples.

The detailed experimental procedure for preparing $NKNS_y$ was reported elsewhere.[18] The samples were poled under a dc electric field of 3 kV/mm for 15 min at room temperature. Temperature dependent dielectric properties of unpoled and poled samples were measured using a LCR meter (E4980A, Agilent, Santa Clara, CA). For ex-situ x-ray measurements, the conductive adhesives were screened on two polished surfaces and then dried. These samples were then poled under the same conditions as mentioned above. In addition, gold electrodes were sputtered onto two major sides for in-situ x-ray measurement. Both ex-situ and in-situ x-ray measurements were taken at beam line 14B1 ($\lambda = 1.2378$ Å) at Shanghai Synchrotron Radiation Facility in a symmetric reflection geometry. Measurements were performed by high-resolution θ-2θ step-scans using a Huber 5021 six-circle diffratometer with a NaI scintillation detector. The angle between the detector and the sample surfaces is θ. For in-situ diffraction measurement, the sample surface was perpendicular to the applied electric field. The beam size at the sample position is about 0.3×0.3 mm. The grain size of the samples for the synchrotron radiation is about 1–5 μm. Therefore, the collected diffraction data would disclose the statistical average structure information.

Figure 1 shows the variation of (200), (220), and (222) pseudocubic reflections for $NKNS_y$ ceramics before and after electric poling by means of synchrotron x-ray diffraction. As seen from Fig. 1(a), the unpoled pure NKN (y = 0) sample exhibits obvious features of an O symmetry, as characterized by the $(202)_o/(020)_o$ doublet, $(004)_o/(400)_o/(222)_o$ triplet, and $(024)_o/(420)_o$ doublet. These features are similar to the O phase observed in $BaTiO_3$ and $Pb(Zn_{1/3}Nb_{2/3})O_3$-$PbTiO_3$.[6]
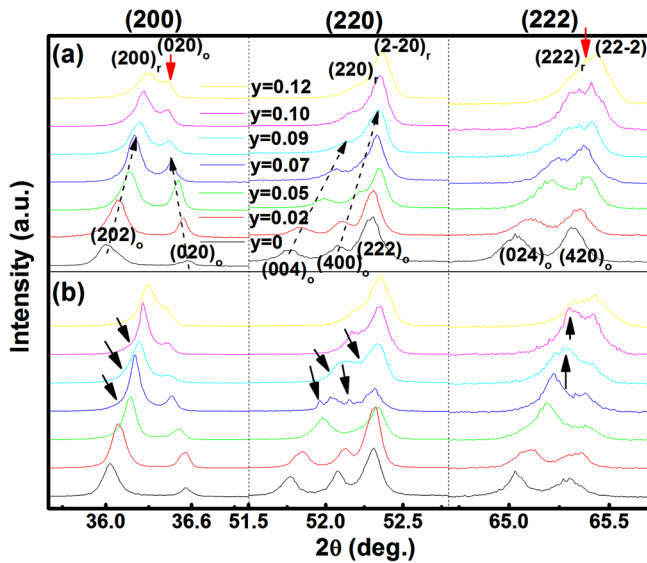
FIG. 1. Synchrotron x-ray diffraction patterns on (200), (220), and (222) pseudocubic reflections for (a) unpoled and (b) poled NKNSy ceramics.

With increasing the Sb content, the orthorhombicity becomes weak gradually as denoted by two arrows. In addition, the initial three peaks around the $(220)_c$ reflection corresponding to the orthorhombic $(004)_o/(400)_o/(222)_o$ triplet gradually merge into two peaks when the Sb content (y) is beyond 0.07, implying that the phase structure tends to transform into an R symmetry. It is known that the R phase is characterized of a single peak corresponding to the $(200)_r$ reflection, and two double-peaks on the $(220)_c$ and $(222)_c$ planes corresponding to the $(220)_r$ and $(2-20)_r$ reflections and $(222)_r$ and $(22-2)_r$ reflections, respectively. However, no single R phase can be distinctly observed even in the sample with y = 0.12, as demonstrated by the presence of the diffraction peaks corresponding to the O phase (as denoted by red arrows in Fig. 1(a)). According to our previous results,[18] the Sb content (y) cannot be further increased because its solubility limit has been reached. Nevertheless, the above results indicate that the coexistence of the O and R phases occurs in a wide composition range of 0.07 < y < 0.12 for unpoled samples. By comparison, both the peak intensity and position of the diffraction profiles show significant changes for all compositions after electric poling, as shown in Fig. 1(b). Compared with unpoled samples, it is found that the intensity ratio of lower to higher angle diffraction peaks of all reflection lines increased, suggesting that electric poling induces a considerable domain reorientation along the electric field direction. Besides, an obvious phase structural transition can be discerned once y ≥ 0.07, as characterized by the appearance of the additional diffraction peaks denoted by black arrows in Fig. 1(b). This new phase can be regarded as neither an O symmetry nor an R symmetry. The result suggests that an IP between R and O phases was irreversibly induced by electric poling. In addition, It is worthy of note that the y = 0.07 sample is just located at the O-rich phase zone near the R-O phase boundary before poling (Fig. 1(a)). Therefore, it can be believed that this IP phase should be irreversibly transformed from the initial O phase. Moreover, the characteristic of the induced IP becomes weak gradually

with further increasing the Sb content. No obvious difference of the diffraction peaks can be found for the y = 0.12 sample before and after poling, further confirming that the IP was induced by the O phase rather than the R phase. As a result, the R-O phase boundary prior to poling in NKNS$_y$ ceramics can be identified in the composition range of y = 0.09–0.12, which becomes an R-IP-O phase boundary after poling. For the x = 0.07-0.08 samples, their phase boundary becomes an IP-O phase boundary after poling.

Figure 2(a) shows the temperature dependence of the dielectric constant of poled NKNS$_y$ samples (y = 0.05-0.12) measured at 1 MHz. It is found that, similar to the unpoled samples, three obvious dielectric anomalies can be observed for y = 0.05, at temperatures denoted by T_1, T_3, and T_c from low to high temperatures. It can be easily deduced that the dielectric anomaly at ∼290 °C for the y = 0.05 sample corresponds to the ferroelectric T-paraelectric cubic (C) phase transition temperature (T_c). The other two dielectric anomalies at ∼150 °C and ∼0 °C should correspond to the O-T and R-O polymorphic phase transitions. There is no detectable irreversible phase structural transition induced by poling in the y = 0.05 sample. As the Sb content is larger than 0.07, in addition to the above-mentioned, three peaks at T_1, T_3, and T_c, one more dielectric anomaly at T_2 can be also distinctly recognized. This abrupt change occurs between y = 0.05 and y = 0.07, keeping good agreement with the XRD results in Fig. 1. To clearly identify the possible phase transition and the implication of the T_1, T_2, and T_3 after poling, the temperature dependence of the dielectric constant and loss tangent of the unpoled and poled sample with y = 0.09 at 1 MHz is shown in Fig. 2(b) for comparison. From Fig. 1, one can find that only part of the O phase was transformed into the IP phase. Therefore, between T_1 and T_2 should be the IP and O zone (Fig. 2(b)). Therefore, four temperatures T_1, T_2, T_3, and T_c can be unambiguously assigned to the R-IP, IP-O, O-T, and T-C phase transition temperatures. It is interesting to note that the O phase zone was evidently shrunk in the poled sample. Moreover, the O-T phase transition temperature was
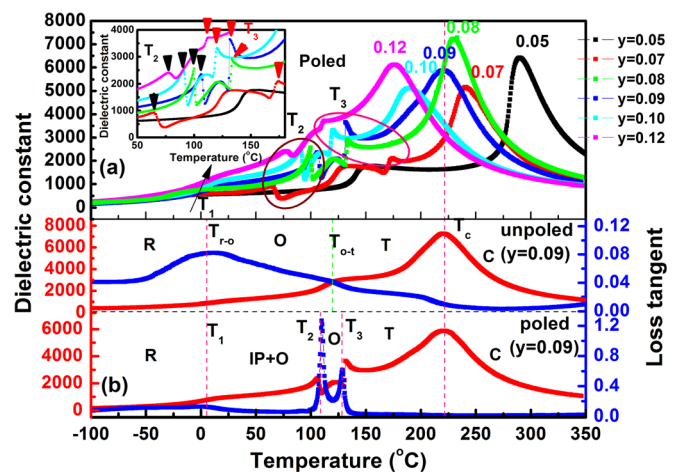

FIG. 2. (a) Dielectric constant of poled NKNSy (y = 0.05–0.12) ceramics measured at 1 MHz as a function of temperature and (b) dielectric constant and loss tangent of unpoled and poled NKNS0.09 samples at 1 MHz as a function of temperature. The inset of Fig. 2(a) is the locally magnified dielectric constant versus temperature curves near T2 and T3 denoted by black and red arrows, respectively.

definitely shifted to higher temperature from the T_{o-t} denoted for the unpoled $y = 0.09$ sample to the T_3 for the poled one. By comparison, one could clearly find that the poling process has almost no effect on the temperature range of low-temperature R phase and high-temperature C phase. That is to say, T_1 (T_{r-o}) and T_c were hardly changed by electric poling. From the inset of Fig. 2(a), T_2 and T_3 for different samples were designated by a few black and red arrows, respectively. It is obvious that T_2 undergoes an increase till the $y = 0.09$ sample and then starts to decrease with further increasing the Sb content, indicating that the induced IP becomes most stable in the $y = 0.09$ sample. However, T_3 exhibits a monotonous decrease with increasing the Sb content. In addition, it can be found from Fig. 2(b) that the T_1 value is nearly independent of the electric poling, meaning that the R phase stability can gradually increase with an increase of the Sb content for both poled and unpoled samples (Fig. 2(a)). Another thing to be noted is that the change of the peak intensity at T_2 shows a similar tendency to the peak position as mentioned above. The peak intensity should be related to the thermal evolution during the phase transition, and is also dominated by the ratio of the induced IP to the remaining O phase. The maximum peak intensity for the poled $y = 0.09$ sample, which owned the optimum piezoelectric and electromechanical properties,[18] implies that IP and O phases reach an appropriate ratio, which leads to the strongest thermal effect during the IP-O phase transition.

The *in-situ* x-ray diffraction results on (200), (220), and (222) pseudocubic reflections of NKNS$_y$ ($y = 0.07$, 0.09, and 0.12) ceramics are shown in Fig. 3. Considering the coercive field value of the samples (0.6–0.4 kV/mm as $y = 0.07$–0.12)[18] and the used poling field value (3 kV/mm), the applied *in-situ* fields were selected between 1 kV/mm and 3 kV/mm. As the applied electric field is zero, the phase structure of the $y = 0.07$ sample is dominated by an O phase, as discussed above. A significant variation of the (200), (220), and (222) pseudocubic diffraction lines can be observed

with increasing the external electric field. Although other diffraction lines also exhibit changes with varying the electric field, the relatively serious peak overlapping would go against the identification of different phases. It can be seen that as the electric field is applied, additional Bragg peaks start to appear and also become more and more obvious with increasing the electric field. These peaks seem to conform to the feature of an M phase with Cm symmetry due to its unique $(111)_c$ triplet instead of the initial R or O phases or the M phase with Pm symmetry, because all these three phases should exhibit an obvious $(111)_c$ doublet.[6,7,10,20] Moreover, one can further deduce that the electric field induced M phase might be an M_B phase with a C_m symmetry on the basis of the relationship between the O, M, and R phases proposed by Vanderbilt and Cohen by using higher-order Devonshire theory,[23] as sketched in the inset of Fig. 3. That is to say, the aforementioned IP could be referred to as an M_B phase. According to the proposed M_B phase model, the peak positions of the induced phase can be calculated by the Bragg law $2d_{hkl}\sin\theta = \lambda$, where λ is the wavelength of the X-ray radiation and d_{hkl} is the interplanar spacing of (hkl) plane. The d_{hkl} is calculated by an M model[24] in which the lattice parameters can be achieved by the peak fitting analysis using a pseudo-Voigt peak shape function and a cell refinement model in Jade 6 software. It can be seen that the calculated peak positions are in good coincidence with the measured ones by using the $y = 0.07$ poled sample as a case study, as shown in Fig. 3. Nevertheless, it is worth noting that the domain texture can be induced by the domain reorientation during poling and the degree of the domain texture increases with increasing the amplitude of the electric field, as indicated by the gradual increase in the intensity of the lower-angle-side peaks in Fig. 3. This means that poling favors the ferroelectric domain orientations with longer c-axis more closely aligned with the electric field direction.[25] However, the intensity of these peaks cannot be completely sustained after removal of the electric field, indicating that the domain texture should not be a saturated state after removal of the electric field (poled state), as seen from the peak intensity change in Fig. 3. Therefore, a precise identification of the new phase structure may need more work using an appropriate scattering geometry setting to minimize the effect of the domain texture.[8] Compared to the diffraction lines of the $y = 0.07$ poled samples, one may find that the featured peaks of the M_B phase could be sustained after removal of the electric field. This further confirms that the electric field induced O-M phase transition is irreversible. Similar changes can be observed in the $y = 0.09$ sample before and after poling, although the virgin samples of $y = 0.09$ and $y = 0.07$ may have different ratios of O and R phases. Compared with the above two samples, the phase structure of the $y = 0.12$ sample prior poling should be composed of an R phase (dominantly) and a small quantity of O phase. As an external electric field is applied on the sample, additional Bragg peaks for an M symmetry can be also induced, as indicated in Fig. 3. However, these peaks cannot be maintained after removal of the electric field (for the poled sample). This means that the electric field induced R-M phase transition is reversible. This point can also be judged from Fig. 2
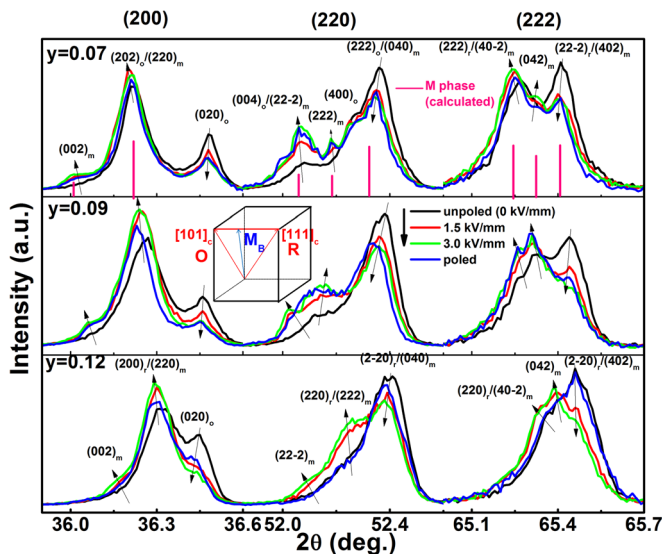

FIG. 3. Evolution of (200), (220), and (222) pseudocubic reflections for the NKNSy ($y = 0.07$, 0.09, and 0.12) samples under different external electric fields. The inset is the sketch of the crystallographic relationship between R and O phase.
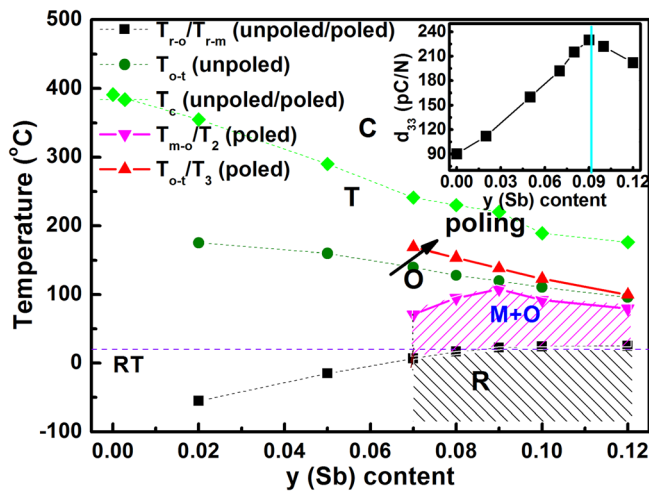
FIG. 4. Phase diagram of poled and unpoled NKNSy ceramics and the inset is the composition dependent piezoelectric properties of NKNSy ceramics.

because the R phase zone was not changed in poled samples (The T_{r-o} value before poling is almost the same as the T_{r-m} (T_1) value). In other words, the O phase instead of R phase tends to be destabilized by an external electric field.

The phase diagram of NKNS$_y$ compositions can be modified after poling, as shown in Fig. 4. The phase zone was indicated by shading for poled samples. It can be seen that the initial R-O phase coexistence around room temperature does not occur any more after poling. Instead, the M-O or R-M-O phase coexistence can be identified near room temperature in the poled ceramics in the composition range of y = 0.07–0.12, depending on the sample composition. Compared with an irreversible M-O phase transition, the reversibility of R-M phase transition tends to cause the phase instability such that the free energy profile in the R-M phase coexistence becomes shallow and flat. Theoretical and experimental studies have suggested that the phase instability and the enhanced piezoelectric response be closely related.[5,26] Most importantly, the electric field induced M phase could allow an easier polarization rotation between the $[101]_O$ and $[111]_R$ polar axes along the (10-1) plane, resulting in the enhancement of the piezoelectric properties and electromechanical properties for NKNS$_y$ ceramics in the proximity of R and O phase coexistence zone, as shown in the inset of Fig. 4. It is interesting to note that the trend of the piezoelectric property in this studied composition range well agrees with the change of the T_{m-o} (T_2), both of which reach the maxima approximately at y = 0.09. This result strongly indicates that the enhancement of the piezoelectric property should be also correlated with the stability of the electric field induced M phase. It is known that the ferroelectric transition sequence in Pb-based ferroelectric single crystals strongly depends on the composition and poling orientation. This finding seems also applicable in NKN-based lead-free ferroelectric ceramics, in which the phase coexistence as well as the electric field induced IP play a basic role in optimizing the path of polarization rotation.[21,22]

In summary, the phase structural transformation in Sb-substituted NKN ceramics was investigated. An intermediate phase with an obvious feature of the M phase was irreversibly induced from the initial O phase under an external electric field. By comparison, the reversibility of the R-M phase transition would induce the phase instability which will make an active contribution to the improved piezoelectric activity as well. Most importantly, the induced M symmetry provides the possibility for optimizing the polarization rotation between the $[101]_O$ and $[111]_R$ polar axes along the (10-1) plane. Moreover, it is also found that the enhanced piezoelectric properties should be also correlated with the stability of the induced M phase.

[1]W. W. Cao and L. E. Cross, Phys. Rev. B **47**, 4825 (1993).
[2]R. Theissmann, L. A. Schmitt, J. Kling, R. Schierholz, K. A. Schonau, H. Fuess, M. Knapp, H. Kungl, and M. J. Hoffmann, J. Appl. Phys. **102**, 024111 (2007).
[3]S.-E. Park and T. R. Shrout, J. Appl. Phys. **82**, 1804 (1997).
[4]N. Yasuda, S. Suzuki, Md. M. Rahman, H. Ohwa, M. Matsushita, Y. Yamashita, M. Iwata, H. Terauchi, and Y. Ishibashi, J. Appl. Phys. **103**, 064509 (2008).
[5]B. Noheda, D. E. Cox, G. Shirane, S.-E. Park, L. E. Cross, and Z. Zhong, Phys. Rev. Lett. **86**, 3891 (2001).
[6]D. E. Cox, B. Noheda, G. Shirane, Y. Uesu, K. Fujishiro, and Y. Yamada, Appl. Phys. Lett. **79**, 400 (2001).
[7]B. Noheda, D. E. Cox, G. Shirane, J. Gao, and Y.-Z. Ye, Phys. Rev. B **66**, 054104 (2002).
[8]M. Hinterstein, J. Rouquette, J. Haines, Ph. Papet, M. Knapp, J. Glaum, and H. Fuess, Phys. Rev. Lett. **107**, 077602 (2011).
[9]R. G. Burkovsky, Yu. A. Bronwald, A. V. Filimonov, A. I. Rudskoy, D. Chernyshov, A. Bosak, J. Hlinka, X. Long, Z.-G. Ye, and S. B. Vakhrushev, Phys. Rev. Lett. **109**, 097603 (2012).
[10]B. Noheda, D. E. Cox, G. Shirane, J. A. Gonzalo, L. E. Cross, and S.-E. Park, Appl. Phys. Lett. **74**, 2059 (1999).
[11]G. Shirane, R. Newnham, and R. Pepinsky, Phys. Rev. **96**, 581 (1954).
[12]Y.-J. Dai, X.-W. Zhang, and K.-P. Chen, Appl. Phys. Lett. **94**, 042905 (2009).
[13]Y. Saito, H. Takao, T. Tani, T. Nonoyama, K. Takatori, T. Homma, T. Nagaya, and M. Nakamura, Nature **432**, 84 (2004).
[14]E. Hollenstein, M. Davis, D. Damjanovic, and N. Setter, Appl. Phys. Lett. **87**, 182905 (2005).
[15]R. Z. Zuo, J. Fu, and D. Y. Lv, J. Am. Ceram. Soc. **92**, 283 (2009).
[16]S. J. Zhang, R. Xia, and T. R. Shrout, Appl. Phys. Lett. **91**, 132913 (2007).
[17]E. K. Akdoğan, K. Kerman, M. Abzari, and A. Safari, Appl. Phys. Lett. **92**, 112908 (2008).
[18]R. Z. Zuo, J. Fu, D. Y. Lv, and Y. Liu, J. Am. Ceram. Soc. **93**, 2783 (2010).
[19]R. Z. Zuo and J. Fu, J. Am. Ceram. Soc. **94**, 1467 (2011).
[20]W. W. Ge, Y. Ren, J. L. Zhang, C. P. Devreugd, J. F. Li, and D. Viehland, J. Appl. Phys. **111**, 103503 (2012).
[21]J. Fu, R. Z. Zuo, S. C. Wu, J. Z. Jiang, L. Li, T. Y. Yang, X. H. Wang, and L. T. Li, Appl. Phys. Lett. **100**, 122902 (2012).
[22]R. Z. Zuo, J. Fu, G. Z. Yin, X. L. Li, and J. Z. Jiang, Appl. Phys. Lett. **101**, 092906 (2012).
[23]D. Vanderbilt and M. H. Cohen, Phys. Rev. B **63**, 094108 (2001).
[24]H. D. Megaw, Proc. Phys. Soc. **58**, 133 (1946).
[25]D. A. Hall, F. Azough, N. Middleton-Stewart, R. J. Cernik, R. Freer, T. Mori, H. Kungl, and C. Curfs, Funct. Mater. Lett. **3**, 31 (2010).
[26]Z. G. Wu and R. E. Cohen, Phys. Rev. Lett. **95**, 037601 (2005).